

# Enhancing Quantum State Reconstruction with Structured Classical Shadows

Zhen Qin,<sup>1,\*</sup> Joseph M. Lukens,<sup>2,3,4,†</sup> Brian T. Kirby,<sup>5,6,‡</sup> and Zhihui Zhu<sup>1,§</sup>

<sup>1</sup>*Department of Computer Science and Engineering, The Ohio State University, Columbus, Ohio 43210, USA*

<sup>2</sup>*Elmore Family School of Electrical and Computer Engineering and Purdue Quantum Science and Engineering Institute, Purdue University, West Lafayette, Indiana 47907, USA*

<sup>3</sup>*Quantum Information Science Section, Oak Ridge National Laboratory, Oak Ridge, Tennessee 37831, USA*

<sup>4</sup>*Research Technology Office and Quantum Collaborative, Arizona State University, Tempe, Arizona 85287, USA*

<sup>5</sup>*DEVCOM Army Research Laboratory, Adelphi, MD 20783, USA*

<sup>6</sup>*Tulane University, New Orleans, LA 70118, USA*

Quantum state tomography (QST) remains the prevailing method for benchmarking and verifying quantum devices; however, its application to large quantum systems is rendered impractical due to the exponential growth in both the required number of total state copies and classical computational resources. Recently, the classical shadow (CS) method has been introduced as a more computationally efficient alternative, capable of accurately predicting key quantum state properties. Despite its advantages, a critical question remains as to whether the CS method can be extended to perform QST with guaranteed performance. In this paper, we address this challenge by introducing a projected classical shadow (PCS) method with guaranteed performance for QST based on Haar-random projective measurements. PCS extends the standard CS method by incorporating a projection step onto the target subspace. For a general quantum state consisting of  $n$  qubits, our method requires a minimum of  $O(4^n)$  total state copies to achieve a bounded recovery error in the Frobenius norm between the reconstructed and true density matrices, reducing to  $O(2^n r)$  for states of rank  $r < 2^n$ —meeting information-theoretic optimal bounds in both cases. For matrix product operator states, we demonstrate that the PCS method can recover the ground-truth state with  $O(n^2)$  total state copies, improving upon the previously established Haar-random bound of  $O(n^3)$ . Simulation results further validate the effectiveness of the proposed PCS method.

## I. INTRODUCTION

Quantum state tomography (QST) is widely used for estimating quantum states [1–5]. To reconstruct the density matrix with high accuracy, measurements should be performed on a large number of identical copies; specifically, for single-copy (i.e., non-collective) measurements, a minimum of  $O(4^n)$  total copies is required to estimate the density matrix of an  $n$ -qubit system with a bounded recovery error, as defined by the Frobenius norm between the reconstructed and true density matrices [6]. Various methods have been proposed to achieve efficient and accurate QST. Classical computational approaches include linear inversion [7], maximum likelihood estimation [4, 5, 8], Bayesian inference [9–11], region estimation [12, 13], classical machine learning [14], and least squares estimators [15–17]. In contrast, quantum machine learning methods encompass algorithms such as variational quantum circuits [18, 19], quantum principal component analysis [20], and quantum variational algorithms combined with classical statistics [21].

A significant reduction in the number of required state copies can be achieved by assuming two common low-dimensional structures: low-rankness and matrix product operators (MPOs). (i) Low-rank density matrices frequently

emerge in quantum systems with pure or nearly pure states that exhibit low entropy [6, 22–25], and low-rank assumptions are employed in various state estimation procedures, with a range of associated measurement processes, including 4-designs [22], Pauli strings [23, 26], Clifford gates [24], and Haar-random projective measurements [25]. When the density matrix has rank  $r$ , the required number of total state copies can be reduced to  $O(2^n r)$  [6, 24], yet this remains exponential in  $n$ , posing challenges for current quantum computers exceeding 100 qubits. (ii) MPOs, on the other hand, offer a more scalable alternative for certain quantum systems, including one-dimensional spatial systems [27], Hamiltonians with decaying long-range interactions [28], and states generated by noisy quantum devices [29]. When employing Haar-random projective measurements [30] or specific classes of informationally complete positive operator-valued measures (IC-POVMs) [31], the required number of total state copies can be reduced to polynomial scaling—either  $O(n^3)$  or  $O(n)$ , respectively—while ensuring bounded recovery error for MPO states.

While algorithms with low-rank assumptions or low-dimensional structures can enable significantly improved scaling, they still face considerable computational complexity, which in existing approaches can be attributed to four potential operations: (i) the calculation of the inverse; (ii) repeated inner product operations between matrices that grow exponentially with  $n$ ; (iii) multiple projection steps onto the target subspace; and (iv) additional matrix multiplications introduced by nonconvex algorithms to enforce low-rankness or MPO representations. Recently, an efficient and experi-

\* qin.660@osu.edu

† jlukens@purdue.edu

‡ brian.t.kirby4.civ@army.mil

§ zhu.3440@osu.edu

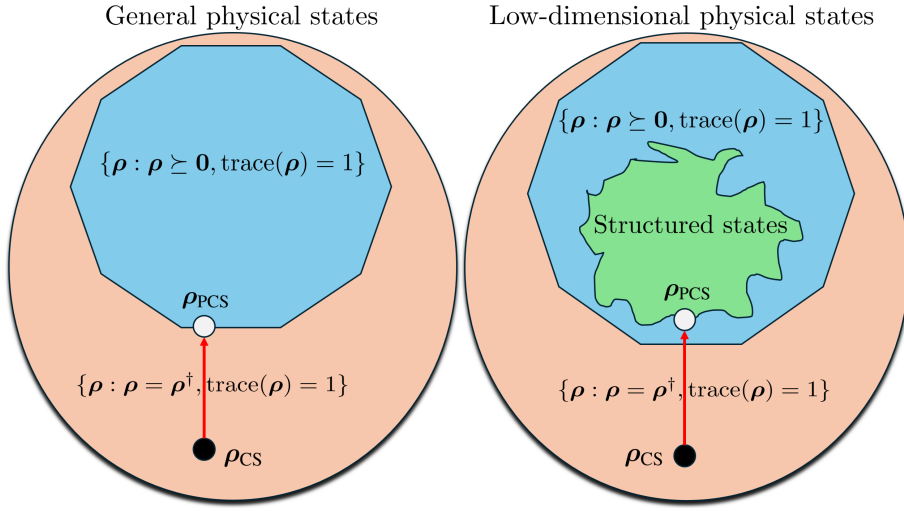


FIG. 1. Illustration of proposed PCS method. Given an initial CS estimate  $\rho_{\text{CS}}$  lying in the space of Hermitian and unit-trace matrices (not necessarily PSD), we compute the closest state  $\rho_{\text{PCS}}$  in the physical space of interest—either the space of all possible states (left) or a subspace possessing a desired structure (right).

mentally feasible approach, known as classical shadow (CS) estimation, was introduced by Ref. [32] to infer limited sets of state properties like fidelity, entanglement measures, and correlations. By exploiting efficient computational and storage capabilities on classical hardware, all necessary processing to predict these properties can be carried out via classical computations. This has sparked a series of studies leveraging the CS method [33–38]. However, existing research predominantly focuses on *state properties*, raising the critical question of whether the CS method can be effectively extended to the *full state* (i.e., QST) with guaranteed performance.

In this paper, we derive performance guarantees for QST using a method we term projected classical shadow (PCS), which projects CS estimators onto target subspaces of the Hilbert space, as illustrated in Fig. 1. Given that the original CS density matrix is Hermitian but not in general positive semidefinite (PSD), our method involves projecting its eigenvalues onto the simplex [39]. We demonstrate that this approach requires  $O(4^n)$  total state copies to achieve a bounded recovery error in the Frobenius norm. For low-rank states, we further leverage (truncated) low-rank eigenvalue decomposition and show that the required number of total state copies can be reduced to  $O(2^n r)$  for the same accuracy. Finally, for MPO states, we employ a quasi-optimal MPO projection—tensor-train singular value decomposition (TT-SVD) [40] with a simplex projection—to form the PCS step, demonstrating that with  $O(n^2)$  total state copies, the method reliably recovers the ground-truth state. While suboptimal relative to the degrees of freedom for MPO states, this approach improves upon the theoretical  $O(n^3)$  scaling in Ref. [30]. PCS also offers a framework for incorporating prior knowledge about the target state form into the CS approach.

*Notation:* We use bold capital letters (e.g.,  $\mathbf{X}$ ) to denote matrices, bold lowercase letters (e.g.,  $\mathbf{x}$ ) to denote column vectors, and italic letters (e.g.,  $x$ ) to denote scalar quantities.

Matrix elements are denoted in parentheses. For example,  $X(i_1, i_2)$  denotes the element in position  $(i_1, i_2)$  of the matrix  $\mathbf{X}$ . The superscripts  $(\cdot)^\top$  and  $(\cdot)^\dagger$  denote the transpose and Hermitian transpose, respectively. For two matrices  $\mathbf{A}, \mathbf{B}$  of the same size,  $\langle \mathbf{A}, \mathbf{B} \rangle = \text{trace}(\mathbf{A}^\dagger \mathbf{B})$  denotes the inner product.  $\|\mathbf{X}\|$ ,  $\|\mathbf{X}\|_1$ , and  $\|\mathbf{X}\|_F$  respectively represent the spectral, trace, and Frobenius norm of  $\mathbf{X}$ . For two positive quantities  $a, b \in \mathbb{R}^+$ , the inequality  $b \lesssim a$  or  $b = O(a)$  implies  $b \leq ca$  for some universal constant  $c$ ; likewise,  $b \gtrsim a$  or  $b = \Omega(a)$  represents  $b \geq ca$  for some universal constant  $c$ .

## II. CLASSICAL SHADOWS

Quantum information science harnesses quantum states for information processing [41]. The state of an  $n$ -qubit system can be described by the density operator  $\rho \in \mathbb{C}^{2^n \times 2^n}$ , which is PSD ( $\rho \succeq 0$ ) and has unit-trace ( $\text{trace}(\rho) = 1$ ). In order to estimate this states, measurements can be performed on a collection of copies.

*Projective measurements:* Within the most general quantum measurement framework of positive operator valued measures (POVMs) [42], the special case of projective measurements is often employed, where the measurement outcomes are associated with an orthonormal eigenbasis of the system. To implement such a measurement defined by an arbitrary orthonormal basis  $\{\phi_k : \phi_k^\dagger \phi_l = \delta_{kl}\}$ , we can introduce a unitary matrix  $\mathbf{U} = [\phi_1 \ \cdots \ \phi_{2^n}] \in \mathbb{C}^{2^n \times 2^n}$  and apply  $\mathbf{U}^\dagger$  to the state  $\rho$  before conducting a projective measurement in the computational basis  $\{e_k\}$ , where  $\mathbf{U} e_k = \phi_k$ . The probability of observing the  $k$ -th outcome is given by:

$$p_k = \langle \phi_k \phi_k^\dagger, \rho \rangle = e_k^\dagger (\mathbf{U}^\dagger \rho \mathbf{U}) e_k. \quad (1)$$

However, a single projective measurement, even if repeated infinitely many times, provides only partial information on

$\rho$ , so multiple projective measurements must be conducted in various bases. In the subsequent discussion, we denote the number of distinct measurement bases by  $M$ , and the measurement operators for the  $m$ -th projective measurement by  $\{\phi_{m,1}\phi_{m,1}^\dagger, \dots, \phi_{m,2^n}\phi_{m,2^n}^\dagger\}$ .

*Classical shadow (CS):* Consider the original CS proposal with single-shot Haar-random projective measurements. Given an unknown  $n$ -qubit ground truth  $\rho^*$ , we repeatedly execute the measurement procedure above Eq. (1) in which  $U$  is chosen randomly from the Haar distribution and each measurement is performed on only one copy (i.e., a new  $U$  is selected for each copy measured). The specific result  $e_{j_m}$  yields a snapshot, or “shadow,” of the underlying quantum state, which for Haar-distributed unitaries can be expressed as [32]:

$$\begin{aligned}\rho_m &= (2^n + 1)U_m e_{j_m} e_{j_m}^\dagger U_m^\dagger - \mathbf{I}_{2^n} \\ &= (2^n + 1)\phi_{m,j_m}\phi_{m,j_m}^\dagger - \mathbf{I}_{2^n}.\end{aligned}\quad (2)$$

By construction, this snapshot equals the ground truth in expectation (over both unitaries and measurement outcomes):  $\mathbb{E}[\rho_m] = \rho^*$ . Executing this process  $M$  times produces an array of  $M$  independent classical snapshots for the total CS estimator:

$$\begin{aligned}\rho_{\text{CS}} &= \frac{1}{M} \sum_{m=1}^M \rho_m \\ &= \frac{1}{M} \sum_{m=1}^M \left[ (2^n + 1)\phi_{m,j_m}\phi_{m,j_m}^\dagger - \mathbf{I}_{2^n} \right].\end{aligned}\quad (3)$$

*CS for Tomography?* Although CS estimators can efficiently predict observables of  $\rho^*$ , to our knowledge there exist no results concerning recovery error of the *full state*. Following the detailed derivation in Appendix A, we find the expectation of the mean squared error:

$$\mathbb{E} \|\rho_{\text{CS}} - \rho^*\|_F^2 = \frac{4^n + 2^n - 1 - \|\rho^*\|_F^2}{M}.\quad (4)$$

Given that  $\|\rho^*\|_F^2 \leq [\text{trace}(\rho^*)]^2 = 1$ , it follows that Eq. (4) can be simplified to

$$\mathbb{E} \|\rho_{\text{CS}} - \rho^*\|_F^2 \approx \frac{4^n}{M}\quad (5)$$

for large  $n$ . Eq. (5) demonstrates that stable recovery of the full state can be achieved only when  $M$  scales proportionally to  $4^n$ , aligning with the optimal  $M$  required in QST for general states [6].

A comparison between CS and traditional QST returns several key observations of relevance to this study:

1. CS yields an unbiased estimate ( $\mathbb{E}[\rho_{\text{CS}}] = \rho^*$ ), whereas the solution from QST is often biased [43].
2. While the CS estimator is typically unphysical (not PSD), leading QST methods like MLE [5], projected least squares [44], and Bayesian inference [9] enforce physicality by construction.

3. CS boasts significantly lower computational complexity compared to QST.
4. For  $M \ll 2^n$ , CS outperforms QST in predicting certain linear observables, not in predicting the entire state [17, 45].
5. Including prior information about state structure allows for a reduction in scaling in QST (see Tables I and II). Currently no known method for similarly reducing CS scaling exists. In other words, CS requires  $O(4^n)$  measurements for estimating the full state, as demonstrated in Eq. (5).

In the next section we investigate methods for incorporating prior information about state structure into CS to reduce the scaling shown in Eq. (5).

### III. PROJECTED CLASSICAL SHADOW (PCS) FOR QST

In this section, we will study the application of CS for the task of describing the full quantum state and show that, with a simple projection step, CS estimators are also effective for QST and achieve (nearly) information-theoretically optimal bounds for broad classes of states. Let  $\mathbb{X}$  denote the class of states of interest, and assume that the underlying ground truth  $\rho^* \in \mathbb{X}$ . For instance,  $\mathbb{X}$  could contain all physical states (PSD and unit-trace) or be restricted to a specific structure with compact representations, such as low-rank or MPO states. We then define  $\rho_{\text{CS}}$  as the projection of  $\rho_{\text{CS}}$  on the set  $\mathbb{X}$  that minimizes Frobenius error, i.e.,

$$\rho_{\text{PCS}} = \mathcal{P}_{\mathbb{X}}(\rho_{\text{CS}}) := \arg \min_{\rho \in \mathbb{X}} \|\rho - \rho_{\text{CS}}\|_F.\quad (6)$$

To provide a unified and general analysis of Eq. (6), we enlist tools from  $\epsilon$ -net and covering number theory to capture the complexity of the classes of states within the set  $\mathbb{X}$ . First, consider the set  $\mathcal{N} = \left\{ \frac{\rho}{\|\rho\|_F} : \rho \in \mathbb{X} \right\}$  scaled to unit Frobenius norm. For  $\epsilon > 0$ , the set  $\mathcal{N}_\epsilon \subset \mathcal{N}$  is said to be an  $\epsilon$ -net (or an  $\epsilon$ -cover) over  $\mathcal{N}$  if for all  $\frac{\rho}{\|\rho\|_F} \in \mathcal{N}$ , there exists  $\frac{\rho'}{\|\rho'\|_F} \in \mathcal{N}_\epsilon$  such that  $\left\| \frac{\rho}{\|\rho\|_F} - \frac{\rho'}{\|\rho'\|_F} \right\|_F \leq \epsilon$ . The size of an  $\epsilon$ -net with the smallest cardinality is called the covering number of  $\mathbb{X}$ , denoted by  $N_\epsilon(\mathbb{X})$ . Intuitively speaking, a covering number is the minimum number of balls of a specified radius  $\epsilon$  to cover a given set entirely. Coverings are useful for managing the complexity of a large set: instead of directly analyzing the behavior of an uncountable number of points in  $\mathcal{N}$ , we can analyze the finite number of points in  $\mathcal{N}_\epsilon$ . The behavior of all points in  $\mathcal{N}$  is similar to that of the points in  $\mathcal{N}_\epsilon$ , as each point in  $\mathcal{N}$  is close to some point in the covering.

Instead of the covering number  $N_\epsilon(\mathbb{X})$ , our analysis will rely on the covering number of the set  $\bar{\mathbb{X}}$  formed by the differences between the elements in  $\mathbb{X}$ :

$$\bar{\mathbb{X}} = \left\{ \rho_1 - \rho_2 : \rho_1, \rho_2 \in \mathbb{X}, \rho_1 \neq \rho_2 \right\}.\quad (7)$$

In many cases, the covering number  $N_\epsilon(\bar{\mathbb{X}})$  can be upper bounded by  $N_\epsilon^2(\bar{\mathbb{X}})$ . Here we use  $\bar{\mathbb{X}}$  for convenience in the following.

The covering number when  $\mathbb{X}$  comprises all physical quantum states can be computed as  $\log N_\epsilon(\bar{\mathbb{X}}) = O(4^n \log \frac{9}{\epsilon})$ . By comparison, for quantum states with rank at most  $r$ , this reduces to  $\log N_\epsilon(\bar{\mathbb{X}}) = O(2^n r \log \frac{9}{\epsilon})$ ; when the density matrices are represented by MPOs with bond dimension  $D$ , the covering number can be further reduced to  $\log N_\epsilon(\bar{\mathbb{X}}) = O(4nD^2 \log \frac{4n+\epsilon}{\epsilon})$ , as discussed in Sec. III.

**Theorem 1.** *For a given  $\rho^* \in \mathbb{X}$ , let  $\rho_{\text{PCS}}$  be the projected CS in Eq. (6). Then with probability at least  $1 - e^{-\Omega(\log N_{1/2}(\bar{\mathbb{X}}))}$ ,*

$$\|\rho_{\text{PCS}} - \rho^*\|_F \leq O\left(\sqrt{\frac{\log N_{1/2}(\bar{\mathbb{X}})}{M}}\right). \quad (8)$$

The proof is given in Appendix B. Here the set  $\mathbb{X} \subset \{\rho \in \mathbb{C}^{2^n \times 2^n} : \rho = \rho^\dagger, \text{trace}(\rho) = 1\}$  is any subspace of Hermitian, trace-one matrices (tan space in Fig. 1). The set  $\mathbb{X}$  will be specialized to PSD matrices only (blue space in Fig. 1) in Corollary 1 and low-dimensional structures (green space in Fig. 1) in Theorems 3 and 4. Theorem 1 guarantees a stable recovery of the ground-truth  $\rho^*$  with  $\xi$ -closeness in the Frobenius norm, provided that the number of Haar-random projective measurements  $M$  satisfies  $M \geq \Omega(\log N_{1/2}(\mathbb{X})/\xi^2)$ , which scales linearly with the logarithm of the covering number. For structured sets  $\mathbb{X}$  that are nonconvex, such as MPO states, computing the optimal projection  $\mathcal{P}_{\mathbb{X}}$  might be difficult or even NP-hard. For these cases, we can use numerical methods to compute an approximate projection  $\tilde{\mathcal{P}}_{\mathbb{X}}$  that we assume is  $\alpha$ -approximately optimal ( $\alpha \geq 1$ ), satisfying

$$\tilde{\mathcal{P}}_{\mathbb{X}}(\rho) \in \mathbb{X}, \quad \left\| \tilde{\mathcal{P}}_{\mathbb{X}}(\rho) - \rho \right\|_F \leq \sqrt{\alpha} \|\mathcal{P}_{\mathbb{X}}(\rho) - \rho\|_F \quad (9)$$

for any  $\rho$ . Denote by  $\tilde{\rho}_{\text{PCS}} = \tilde{\mathcal{P}}_{\mathbb{X}}(\rho_{\text{PCS}})$  the PCS estimator obtained with this approximate projection. The following extends the results in Theorem 1 to  $\tilde{\rho}_{\text{PCS}}$ .

**Theorem 2.** *For a given  $\rho^* \in \mathbb{X}$ , let  $\tilde{\rho}_{\text{PCS}}$  be the approximate PCS estimator in Eq. (9). Then with probability at least  $1 - e^{-\Omega(\log N_{1/2}(\bar{\mathbb{X}}))}$ ,*

$$\|\tilde{\rho}_{\text{PCS}} - \rho^*\|_F \leq O\left(\sqrt{\frac{\alpha \log N_{1/2}(\bar{\mathbb{X}})}{M}}\right). \quad (10)$$

### General physical states

We first specialize  $\mathbb{X}$  to all physical quantum states [46]:

$$\mathbb{X}_{\text{simplex}} = \{\rho \in \mathbb{C}^{2^n \times 2^n} : \rho \succeq \mathbf{0}, \text{trace}(\rho) = 1\}. \quad (11)$$

For  $\mathbb{X}_{\text{simplex}}$ , we can achieve the PCS projection in Eq. (6) by performing an eigenvalue decomposition and projecting the eigenvalues to the simplex after the algorithm of

Ref. [44]. Since the corresponding set  $\bar{\mathbb{X}}$  has covering number  $\log N_\epsilon(\bar{\mathbb{X}}) = O(4^n \log \frac{9}{\epsilon})$ , we can plug this information into Theorem 1 to obtain recovery guarantee for  $\mathcal{P}_{\text{simplex}}(\rho_{\text{CS}})$ .

**Corollary 1.** *For a given physical state  $\rho^* \in \mathbb{C}^{2^n \times 2^n}$ , we perform  $M$  projective measurements to obtain the CS estimate  $\rho_{\text{CS}}$ . Then with probability at least  $1 - e^{-\Omega(4^n)}$ , the projected classical shadow  $\mathcal{P}_{\text{simplex}}(\rho_{\text{CS}})$  satisfies*

$$\|\mathcal{P}_{\text{simplex}}(\rho_{\text{CS}}) - \rho^*\|_F \leq O\left(\sqrt{\frac{4^n}{M}}\right). \quad (12)$$

### Low-rank states

We next explore the structure of pure or nearly pure quantum states characterized by low entropy and represented as low-rank density matrices. Assuming  $\rho^*$  has rank  $r \leq 2^n$ , we can refine our attention to the set  $\mathbb{X}_r = \{\rho \in \mathbb{C}^{2^n \times 2^n} : \rho \succeq \mathbf{0}, \text{trace}(\rho) = 1, \text{rank}(\rho) = r\}$ . Denote  $\mathcal{P}_{\mathbb{X}_r}(\cdot)$  as the optimal projection satisfying Eq. (6). It follows from Theorem 1 and the covering number of the corresponding set  $\log N_\epsilon(\bar{\mathbb{X}}) = O(2^n r \log \frac{9}{\epsilon})$  that  $\|\mathcal{P}_{\mathbb{X}_r}(\rho_{\text{CS}}) - \rho^*\|_F \leq O(\sqrt{2^n r / M})$ .

However, since we are unaware of an algorithm to perform the ideal projection  $\mathcal{P}_{\mathbb{X}_r}(\cdot)$ , we instead consider a two-step alternative to obtain the low-rank projected classical shadow (LR-PCS):

$$\rho_{\text{LR-PCS}} = \mathcal{P}_{\text{simplex}}(\mathcal{P}_{\text{rank-}r}(\rho_{\text{CS}})), \quad (13)$$

where  $\mathcal{P}_{\text{rank-}r}(\cdot)$  denotes the rank- $r$  projection obtained by setting all eigenvalues beyond the  $r$ -th largest eigenvalue to zero. We can show that  $\rho_{\text{LR-PCS}}$  shares a similar guarantee as  $\mathcal{P}_{\mathbb{X}_r}(\rho_{\text{CS}})$ .

**Theorem 3.** *Given  $M$  Haar-random projective measurements on physical state  $\rho^* \in \mathbb{X}_r$ , with probability  $1 - e^{-\Omega(2^n r)}$   $\rho_{\text{LR-PCS}}$  defined in Eq. (13) satisfies*

$$\|\rho_{\text{LR-PCS}} - \rho^*\|_F \leq O\left(\sqrt{\frac{2^n r}{M}}\right). \quad (14)$$

The detailed proof appears in Appendix C. This theoretical recovery error is optimal, given that the degrees of freedom for the ground truth  $\rho^*$  are  $O(2^n r)$ . This highlights that LR-PCS can achieve the optimal solution in QST using independent measurements, without requiring multiple iterations of optimization algorithms.

To compare LR-PCS with prior results, we convert the result of Theorem 3 to trace norm leveraging the inequality between the Frobenius and the trace norms [6], namely  $\|\rho_{\text{LR-PCS}} - \rho^*\|_1 \leq \sqrt{2r} \|\rho_{\text{LR-PCS}} - \rho^*\|_F \leq O(\sqrt{2^n r^2 / M})$ , which matches the optimal guarantee (up to small log terms) with independent measurements according to [6]. We have summarized the comparison in Table I.

TABLE I. Comparing the total number of state copies in PCS using single-shot global Haar unitaries to that in optimal QST. Here,  $n$  denotes the number of qubits,  $r$  represents the rank of the target state, and  $\xi$  signifies the desired precision in trace distance, i.e.,  $\|\hat{\rho} - \rho^*\|_1 \leq \xi$  for estimator  $\hat{\rho}$ .

Methods	$\rho^* \in \mathbb{X}_{\text{simplex}}$	$\rho^* \in \mathbb{X}_r$
PCS	$\Omega(8^n/\xi^2)$	$\Omega(2^n r^2/\xi^2)$
Optimal QST [6]	$\Omega(8^n/\xi^2)$	$\Omega(2^n r^2/(\xi^2 \log(1/\xi)))$

### MPO states

While the computational and storage requirements for low-rank density matrices are significantly smaller compared to general ones, they still grow exponentially in the number of qubits  $n$ . Moreover, the assumption of high purity on which the low-rank approximation is based becomes increasingly tenuous in practice for existing processors in the noisy intermediate-scale quantum (NISQ) era. For this reason, reducing parameter count through alternative assumptions is worth pursuing. Examples such as ground states of many quantum systems with short-range interactions and states generated by such systems within a finite duration [27] often possess entanglement localized to subsystems of the entire quantum computer. Consequently, they can be compactly represented using MPOs, whose degrees of freedom scale only polynomially in  $n$ . To assist in the development of an MPO-PCS method, we will first establish their connection to tensor train (TT) decompositions [40], a technique widely utilized in signal processing and machine learning.

For a  $n$ -qubit density matrix  $\rho^* \in \mathbb{C}^{2^n \times 2^n}$ , we employ a single index array  $i_1 \cdots i_n (j_1 \cdots j_n)$  to denote the row (column) indices, where  $i_1, \dots, i_n \in \{1, 2\}$  [47]. We designate  $\rho^*$  as an MPO if we can represent its  $(i_1 \cdots i_n, j_1 \cdots j_n)$ -th element using the following matrix product [48]:

$$\rho^*(i_1 \cdots i_n, j_1 \cdots j_n) = \mathbf{X}_1^{i_1, j_1} \mathbf{X}_2^{i_2, j_2} \cdots \mathbf{X}_n^{i_n, j_n}, \quad (15)$$

where  $\mathbf{X}_\ell^{i_\ell, j_\ell} \in \mathbb{C}^{D \times D}$  for  $\ell \in \{2, \dots, n-1\}$ ,  $\mathbf{X}_1^{i_1, j_1} \in \mathbb{C}^{1 \times D}$ ,  $\mathbf{X}_n^{i_n, j_n} \in \mathbb{C}^{D \times 1}$ , and  $D$  is the *bond dimension*, and thus we can introduce the set of physical MPO states with bond dimension  $D$  as

$$\mathbb{X}_D = \left\{ \rho \in \mathbb{C}^{2^n \times 2^n} : \rho \succeq 0, \text{trace}(\rho) = 1, \text{bond dimension}(\rho) = D \right\}. \quad (16)$$

Here the corresponding difference set  $\overline{\mathbb{X}}$  has covering number  $\log N_\epsilon(\overline{\mathbb{X}}) = O(4nD^2 \log \frac{4n+\epsilon}{\epsilon})$ , which is proportional to the degrees of freedom  $O(4nD^2)$  in the MPO states. Given the optimal projection  $\mathcal{P}_{\mathbb{X}_D}(\cdot)$ , it follows from Theorem 1 that  $\|\mathcal{P}_{\mathbb{X}_D}(\rho_{\text{CS}}) - \rho^*\|_F \leq O(\sqrt{nD^2 \log n/M})$ .

However, we have been unable to implement the optimal  $\mathcal{P}_{\mathbb{X}_D}(\cdot)$  due to the difficulty in satisfying both the MPO and

simplex conditions simultaneously. Therefore, we introduce a quasi-optimal projection based on a sequential singular value decomposition (SVD) algorithm, commonly referred to as tensor train SVD (TT-SVD) [40]. Based on tensor-matrix equivalence, we can design a two-step MPO PCS method:

$$\rho_{\text{MPO-PCS}} = \mathcal{P}_{\text{simplex}}(\text{SVD}_D^{tt}(\rho_{\text{CS}})), \quad (17)$$

where  $\text{SVD}_D^{tt}(\cdot)$  denotes the TT-SVD operation. It is worth noting that the bond dimension of  $\rho_{\text{MPO-PCS}}$  may differ slightly from  $D$  due to the simplex projection, but the recovery error still depends on  $D$ . We analyze the recovery error of Eq. (17) as follows:

**Theorem 4.** Consider an MPO state  $\rho^* \in \mathbb{X}_D$ , measured  $M$  times with Haar-random projections. With  $\rho_{\text{MPO-PCS}}$  defined as in Eq. (17), with probability  $1 - e^{-\Omega(nD^2 \log n)}$  we have

$$\|\rho_{\text{MPO-PCS}} - \rho^*\|_F \leq O\left(\sqrt{\frac{n^2 D^2 \log n}{M}}\right). \quad (18)$$

The proof can be found in Appendix D. Note that due to the quasi-optimality of the TT-SVD, the upper bound of Eq. (18) is not optimal when considering the degrees of freedom  $O(4nD^2)$  in  $\rho^*$ . To our knowledge, there exists no method that can guarantee both MPO and PSD constraints simultaneously. Should such an optimal MPO projection be found, however, we could potentially remove one factor of  $n$  in the numerator of Eq. (18), thus ensuring exact MPO rank. In Table II, we summarize the total number of state copies required for MPO-PCS compared to existing QST methods. It is important to highlight that the QST results represent sufficient, rather than necessary, conditions. Compared with these results, MPO-PCS still demonstrates favorable performance.

TABLE II. Total number of copies in MPO-PCS compared to MPO-based QST using Haar measures, and spherical 3-designs. Here,  $n$  denotes the number of qubits, and  $\zeta$  signifies the desired precision in Frobenius distance, i.e.,  $\|\hat{\rho} - \rho^*\|_F \leq \zeta$  for estimator  $\hat{\rho}$ .

Method	$\rho \in \mathbb{X}_D$
Approximate PCS (Haar)	$\Omega(n^2 D^2 \log n/\zeta^2)$
Optimal PCS (Haar)	$\Omega(nD^2 \log n/\zeta^2)$
QST (Haar) [30]	$\Omega(n^3 D^2 \log n/\zeta^2)$
QST (spherical 3-designs) [31]	$\Omega(nD^2 \log n/\zeta^2)$

## IV. SIMULATION RESULTS

In this section, we conduct numerical QST experiments with Haar-random projective measurements to compare CS, LR-PCS, and MPO-PCS methods. For each configuration, we conduct 10 Monte Carlo tomographic experiments in which each Haar measurement and result are sampled at random; then we take the average over all 10 trials to report the results.

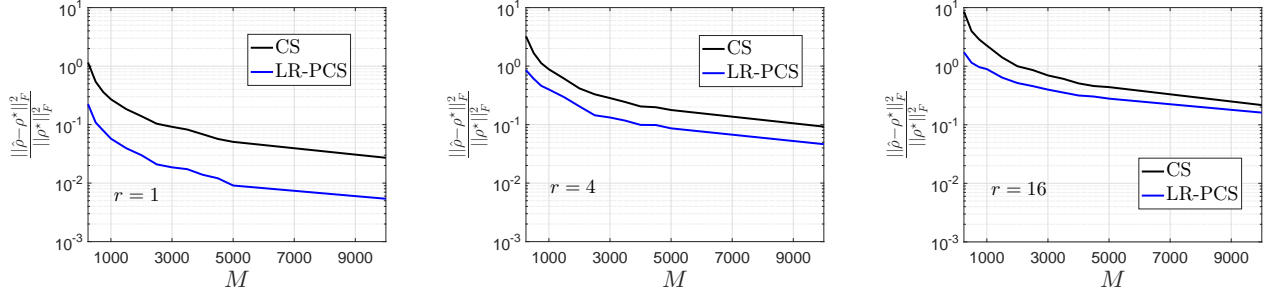


FIG. 2. Mean squared error as a function of state copies  $M$  for CS and LR-PCS methods on  $n = 4$  qubits, averaged over trials on ten randomly chosen ground truth states for each rank  $r \in \{1, 4, 16\}$ . The figures span  $M = 250$  to  $M = 10000$ .

For the random state cases (Figs. 2,3), each trial corresponds to a different randomly chosen ground truth, whereas for the tailored state cases (Figs. 4,5), each trial in a given average is performed on the same ground truth.

In the first set of tests, we compare CS and LR-PCS for a specific rank  $r$  as a function of measurements  $M$ . We generate random ground-truth density matrices  $\rho^* = \mathbf{F}^* \mathbf{F}^{*\dagger} \in \mathbb{C}^{16 \times 16}$  ( $n = 4$  qubits), where  $\mathbf{F}^* = \frac{\mathbf{A}^* + i\mathbf{B}^*}{\|\mathbf{A}^* + i\mathbf{B}^*\|_F} \in \mathbb{C}^{16 \times r}$ , and the entries of  $\mathbf{A}^*$  and  $\mathbf{B}^*$  are independent and identically distributed (i.i.d.) samples drawn from the standard normal distribution. Notably, when  $r = 16$ , LR-PCS reduces to projection onto the set of general physical states defined in Eq. (11). The results in Fig. 2 for rank  $r \in \{1, 4, 16\}$  reveal two key observations: (i) as the rank  $r$  decreases and the number of measurements  $M$  increases, the recovery error across all methods consistently reduces, with the squared error quantitatively scaling as expected ( $4^n/M$  for CS and  $2^n r/M$  for LR-PCS); and (ii) for any  $r$  and  $M$ , LR-PCS outperforms standard CS (even at full rank), as it preserves physicality under any rank constraints.

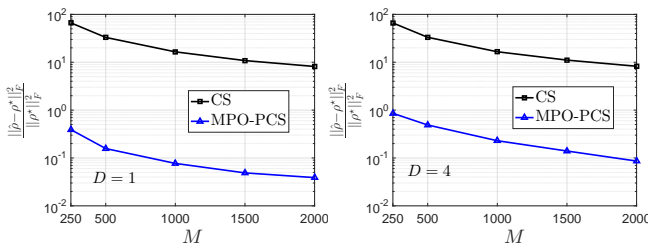


FIG. 3. Mean squared error as a function of state copies  $M$  for CS and MPO-PCS methods on seven-qubit MPO states, where each point is an average over trials on ten randomly chosen ground truth states for each bond dimension  $D \in \{1, 4\}$ .

In the second set of trials, we test CS and MPO-PCS across varying numbers of measurements  $M$  and bond dimension  $D$ . We consider  $n = 7$ -qubit matrix product states (MPSs, pure

state special cases of MPOs) of the form  $\rho^* = \mathbf{u}^* \mathbf{u}^{*\dagger} \in \mathbb{C}^{128 \times 128}$ , where  $\mathbf{u}^* \in \mathbb{C}^{128 \times 1}$  satisfies  $\|\mathbf{u}^*\|_2 = 1$  and its  $(i_1 \cdots i_7)$ -element can be represented in the matrix product form:  $\mathbf{u}^*(i_1 \cdots i_7) = \mathbf{U}_1^{*i_1} \cdots \mathbf{U}_7^{*i_7}$ . Here, each matrix  $\mathbf{U}_\ell^{*i_\ell}$  has size  $d \times d$ , except for  $\mathbf{U}_1^{*i_1}$  and  $\mathbf{U}_7^{*i_7}$  of dimensions of  $1 \times d$  and  $d \times 1$ , respectively.

To generate each MPS  $\mathbf{u}^*$ , we draw a length-128 complex vector with i.i.d. standard normal elements, apply TT-SVD [40] to truncate it to an MPS, and then normalize the result to unit length. As a result, entry  $\rho^*(i_1 \cdots i_7, j_1 \cdots j_7)$  can be expressed as  $\rho^*(i_1 \cdots i_7, j_1 \cdots j_7) = (\mathbf{U}_1^{*i_1} \otimes \mathbf{U}_1^{*j_1\dagger}) \cdots (\mathbf{U}_7^{*i_7} \otimes \mathbf{U}_7^{*j_7\dagger}) = \mathbf{X}_1^{*i_1, j_1} \cdots \mathbf{X}_7^{*i_7, j_7}$ , where  $\otimes$  denotes the Kronecker product. Thus,  $\rho^* = \mathbf{u}^* \mathbf{u}^{*\dagger}$  is also an MPO with bond dimension  $D = d^2$  (equal for all qubits). As shown in Fig. 3 MPO-PCS attains significantly lower error than CS, as it leverages knowledge about the underlying MPO structure. And the recovery error of MPO-PCS increases with higher MPO bond dimension (in line with Table II), whereas that of CS remains the same regardless of  $D$ .

In the third set of trials, we simulate measurements on 7-qubit density matrices: (i) thermal state [49] with temperature  $T = 0.2$  (a relatively low temperature close to the ground state); (ii) thermal state with temperature  $T = 2$  (corresponding to a relatively high temperature); and (iii) Greenberger–Horne–Zeilinger (GHZ) state [50]. It is worth noting that the low-temperature thermal state (i) and the GHZ state (iii) simultaneously exhibit low-rank and MPO structures [24, 51, 52], making them well-suited for demonstrating the advantages of exploiting structured subspaces. We impose a rank constraint  $r \in \{4, 24, 1\}$  for the estimator on each state, respectively. For the  $T = 0.2$  thermal state, the ground-truth density matrix has rank of approximately 4, while for the high-temperature case ( $T = 2$ ), it is full-rank; for LR-PCS  $r = 24$  is selected, somewhat arbitrarily, which is sufficient to encompass 80% of the sum of the eigenvalues of the ground-truth density matrix. In addition, we apply TT-SVD on the CS estimator to adaptively select the bond dimensions using the error tolerance  $10^{-14}$ . Figure 4 shows that the proposed LR-PCS and MPO-PCS methods outperform standard CS, as quantified by the Frobenius norm. Additionally, MPO-PCS demonstrates superior performance compared to LR-PCS, which can be attributed to the lower degrees of free-

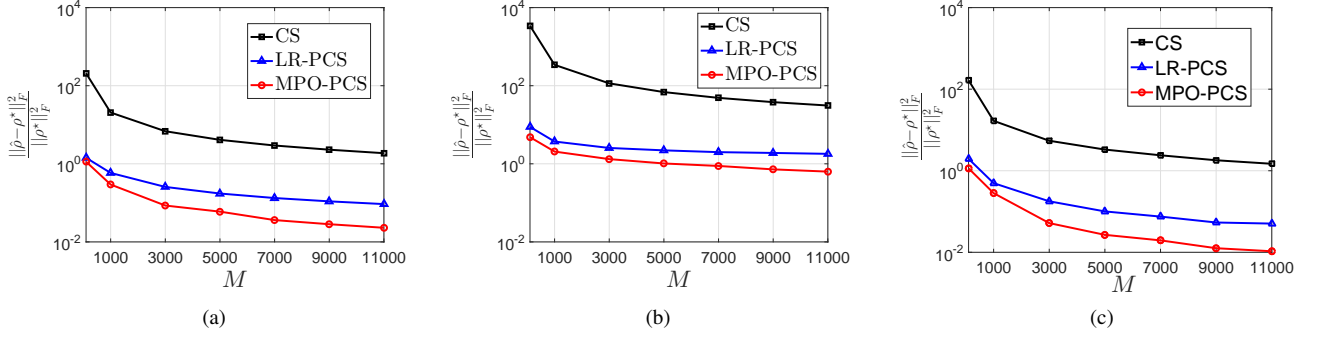


FIG. 4. Mean square error as a function of the number of state copies  $M$  for (a) thermal state ( $T = 0.2$ ), (b) thermal state ( $T = 2$ ), and (c) GHZ state. Comparison between different methods for (a) thermal state ( $T = 0.2$ ), (b) thermal state ( $T = 2$ ), and (c) GHZ state. All figures have  $M = 100$  as the starting point.

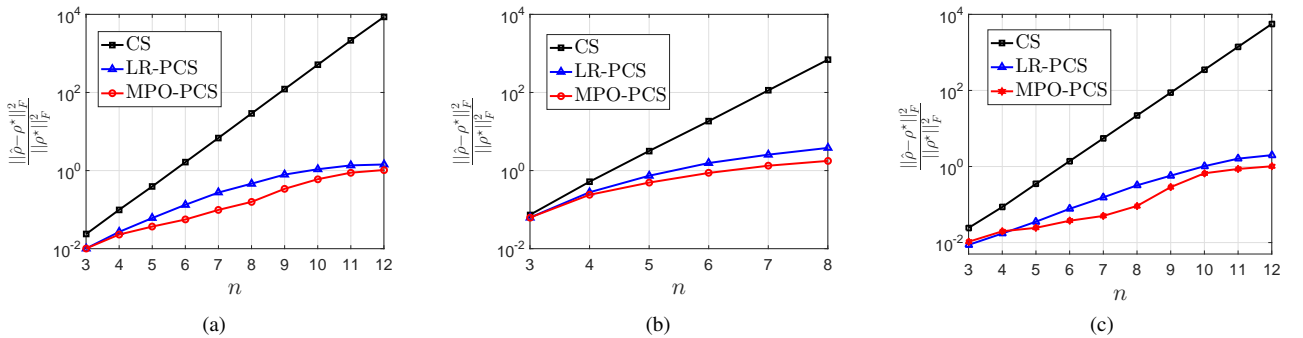


FIG. 5. Mean squared error as a function of the total qubit number with  $M = 3000$  for (a) thermal state ( $T = 0.2$ ), (b) thermal state ( $T = 2$ ), and (c) GHZ state.

dom in the MPO structure relative to the low-rank structure [cf. Eqs. (14,18)].

In the final test, we examine how the recovery error scales with qubit number  $n$ , using parameter settings of  $r = 4$  for  $T = 0.2$ ,  $r = 4(n - 1)$  for  $T = 2$ ,  $r = 1$  for GHZ state and an error tolerance of  $10^{-14}$  for determining bond dimension  $D$ . As highlighted in Fig. 5, both LR-PCS and MPO-PCS effectively attenuate the growth in recovery error as the system size  $n$  increases, in contrast to the standard CS method. This improvement is attributed to the utilization of the low-dimensional structure in these methods. Additionally, the recovery error of MPO-PCS scales polynomially with  $n$ , as indicated in Eq. (18), rather than exponentially as in Eq. (14) of LR-PCS; hence, MPO-PCS outperforms LR-PCS in terms of recovery error.

## V. CONCLUSION

This paper has introduced the projected classical shadow (PCS) method to address the computational challenges of quantum state tomography (QST) in large Hilbert spaces by leveraging the classical shadow (CS) framework combined with a physical projection step. The method provides guar-

anteed performance under Haar-random measurements. Theoretical results show that the PCS method achieves high accuracy in reconstructing general and low-rank quantum states while minimizing the number of state copies, meeting information-theoretically optimal bounds. Moreover, the PCS method reduces the number of state copies required for matrix product operator (MPO) states compared to existing results using Haar random measurements. Numerical validation further demonstrates the practicality and computational efficiency of PCS for large-scale quantum state reconstruction.

More broadly, our formalism points to a promising new general direction for CS methods. Although originally introduced for the estimation of state *properties* rather than the state *per se* [32], CS nevertheless relies on an estimator  $\rho_{\text{CS}}$  of the full density matrix. As our results reveal, this generally unphysical estimator can be projected onto a physical space of interest—whether the entire Hilbert space or some subset thereof (Fig. 1)—with performance guarantees that attain information-theoretic bounds (for the case of arbitrary and low-rank states) or improve upon previous scaling results (for MPO states). Therefore in merging the conceptual simplicity of CS with the scaling improvements possible in structured quantum systems, our results suggest a compelling role for PCS in traditional quantum state estimation, with exciting opportunities for future exploration in even more types of sub-

spaces tailored to specific physical conditions or prior knowledge, such as projected entangled pair operator (PEPO) [53] and multiscale entanglement renormalization ansatz (MERA) [54].

## ACKNOWLEDGMENTS

We acknowledge funding support from the National Science Foundation (CCF-2241298, EECS-2409701) and the

U.S. Department of Energy (ERKJ432, DE-SC0024257). We thank the Ohio Supercomputer Center for providing the computational resources and the Quantum Collaborative led by Arizona State University for providing valuable expertise and resources. A portion of this work was performed at Oak Ridge National Laboratory, operated by UT-Battelle for the U.S. Department of Energy under Contract No. DE-AC05-00OR22725.

---

[1] J. Bertrand and P. Bertrand, *Foundations of Physics* **17**, 397 (1987).

[2] K. Vogel and H. Risken, *Physical Review A* **40**, 2847 (1989).

[3] U. Leonhardt, *Physical review letters* **74**, 4101 (1995).

[4] Z. Hradil, *Physical Review A* **55**, R1561 (1997).

[5] D. F. V. James, P. G. Kwiat, W. J. Munro, and A. G. White, *Phys. Rev. A* **64**, 052312 (2001).

[6] J. Haah, A. Harrow, Z. Ji, X. Wu, and N. Yu, *IEEE Transactions on Information Theory* **63**, 5628 (2017).

[7] U. Fano, *Reviews of modern physics* **29**, 74 (1957).

[8] J. Řeháček, Z. Hradil, and M. Ježek, *Physical Review A* **63**, 040303 (2001).

[9] R. Blume-Kohout, *New Journal of Physics* **12**, 043034 (2010).

[10] C. Granade, J. Combes, and D. Cory, *new Journal of Physics* **18**, 033024 (2016).

[11] J. M. Lukens, K. J. Law, A. Jasra, and P. Lougovski, *New Journal of Physics* **22**, 063038 (2020).

[12] R. Blume-Kohout, *arXiv:1202.5270* (2012).

[13] P. Faist and R. Renner, *Physical review letters* **117**, 010404 (2016).

[14] S. Lohani, B. T. Kirby, M. Brodsky, O. Danaci, and R. T. Glasser, *Machine Learning: Science and Technology* **1**, 035007 (2020).

[15] A. Kyriolidis, A. Kalle, D. Park, S. Bhojanapalli, C. Caramanis, and S. Sanghavi, *npj Quantum Information* **4**, 1 (2018).

[16] F. G. Brandão, R. Kueng, and D. S. França, *arXiv preprint arXiv:2009.08216* (2020).

[17] Z. Zhu, J. M. Lukens, and B. T. Kirby, *Quantum* **8**, 1455 (2024).

[18] P. Sen, A. S. Bhatia, K. S. Bhangu, and A. Elbeltagi, *Plos one* **17**, e0262346 (2022).

[19] Y. Liu, D. Wang, S. Xue, A. Huang, X. Fu, X. Qiang, P. Xu, H.-L. Huang, M. Deng, C. Guo, *et al.*, *Physical Review A* **101**, 052316 (2020).

[20] S. Lloyd, M. Mohseni, and P. Rebentrost, *Nature physics* **10**, 631 (2014).

[21] M. K. Kurmapu, “Machine learning assisted quantum state tomography,” (2020).

[22] R. Kueng, H. Rauhut, and U. Terstiege, *Appl. Comput. Harmon. Anal.* **41**, 88 (2017).

[23] M. Guță, J. Kahn, R. Kueng, and J. A. Tropp, *Journal of Physics A: Mathematical and Theoretical* **53**, 204001 (2020).

[24] F. G. Brandão, R. Kueng, and D. S. França, *arXiv preprint arXiv:2009.08216* (2020).

[25] V. Voroninski, *arXiv preprint arXiv:1309.7669* (2013).

[26] Y.-K. Liu, *Advances in Neural Information Processing Systems* **24** (2011).

[27] J. Eisert, M. Cramer, and M. B. Plenio, *Rev. Mod. Phys.* **82**, 277 (2010).

[28] B. Pirvu, V. Murg, J. I. Cirac, and F. Verstraete, *New Journal of Physics* **12**, 025012 (2010).

[29] K. Noh, L. Jiang, and B. Fefferman, *Quantum* **4**, 318 (2020).

[30] Z. Qin, C. Jameson, Z. Gong, M. B. Wakin, and Z. Zhu, *IEEE Transactions on Information Theory* **70**, 5030 (2024).

[31] Z. Qin, C. Jameson, A. Goldar, M. B. Wakin, Z. Gong, and Z. Zhu, *arXiv preprint arXiv:2410.02583* (2024).

[32] H.-Y. Huang, R. Kueng, and J. Preskill, *Nature Physics* **16**, 1050 (2020).

[33] A. Acharya, S. Saha, and A. M. Sengupta, *Physical Review A* **104**, 052418 (2021).

[34] G. Struchalin, Y. A. Zagorovskii, E. Kovlakov, S. Straupe, and S. Kulik, *PRX Quantum* **2**, 010307 (2021).

[35] A. A. Akhtar, H.-Y. Hu, and Y.-Z. You, *Quantum* **7**, 1026 (2023).

[36] D. Grier, H. Pashayan, and L. Schaeffer, *Quantum* **8**, 1373 (2024).

[37] M. Ippoliti, *Quantum* **8**, 1293 (2024).

[38] S. Becker, N. Datta, L. Lami, and C. Rouzé, *IEEE Transactions on Information Theory* (2024).

[39] Y. Chen and X. Ye, *arXiv preprint arXiv:1101.6081* (2011).

[40] I. Oseledets, *SIAM Journal on Scientific Computing* **33**, 2295 (2011).

[41] M. A. Nielsen and I. L. Chuang, Cambridge (2000).

[42] Specifically, a POVM is characterized as a set of PSD matrices:  $\{\mathbf{A}_1, \dots, \mathbf{A}_K\} \in \mathbb{C}^{2^n \times 2^n}$ , s. t.  $\sum_{k=1}^K \mathbf{A}_k = \mathbf{I}_{2^n}$ . Each POVM element  $\mathbf{A}_k$  corresponds to a potential outcome of a quantum measurement with the special case of projective measurements corresponding to the case where all  $\mathbf{A}_k$  are pairwise orthogonal projection operators, meaning they satisfy  $\mathbf{A}_k^2 = \mathbf{A}_k$  and  $\mathbf{A}_k \mathbf{A}_j = 0$  for  $k \neq j$ .

[43] C. Schwemmer, L. Knips, D. Richart, H. Weinfurter, T. Moroder, M. Kleinmann, and O. Gühne, *Physical review letters* **114**, 080403 (2015).

[44] J. A. Smolin, J. M. Gambetta, and G. Smith, *Physical review letters* **108**, 070502 (2012).

[45] J. M. Lukens, K. J. Law, and R. S. Bennink, *npj Quantum Information* **7**, 113 (2021).

[46] We chose the label “simplex” for this set since the eigenvalues  $\{\lambda_k\}$  of all physical states define a standard simplex, i.e.,  $\lambda_k \geq 0$  and  $\sum_k \lambda_k = 1$ .

[47] Specifically,  $i_1 \cdots i_n$  represents the  $(i_1 + \sum_{\ell=2}^n 2^{\ell-1}(i_\ell - 1))$ -th row.

[48] A. H. Werner, D. Jasczke, P. Silvi, M. Kliesch, T. Calarco, J. Eisert, and S. Montangero, *Physical review letters* **116**, 237201 (2016).

[49] The thermal state is generated from the 1D quantum Ising model  $H = \sum_{j=1}^{n-1} \sigma_j^z \sigma_{j+1}^z + \sum_{j=1}^n \sigma_j^x$  with  $\sigma_j^a = \mathbf{I}_{2^{j-1}} \otimes \sigma^a \otimes \mathbf{I}_{2^{n-j}} \in \mathbb{R}^{2^n \times 2^n}$ ,  $a = x, z$  and  $\sigma^x = \begin{bmatrix} 0 & 1 \\ 1 & 0 \end{bmatrix}$ ,  $\sigma^z = \begin{bmatrix} 1 & 0 \\ 0 & -1 \end{bmatrix}$ . The thermal state is then defined as  $\rho^* = \frac{e^{-H/T}}{\text{trace}(e^{-H/T})}$ .

[50] The GHZ state is constructed as  $\rho^* = gg^\dagger$  where  $g = \begin{bmatrix} \frac{1}{\sqrt{2}} & 0 & \cdots & 0 & \frac{1}{\sqrt{2}} \end{bmatrix}^\top \in \mathbb{R}^{2^n \times 1}$ .

[51] M. Cramer, M. B. Plenio, S. T. Flammia, R. Somma, D. Gross, S. D. Bartlett, O. Landon-Cardinal, D. Poulin, and Y.-K. Liu, *Nature communications* **1**, 1 (2010).

[52] C. Jameson, Z. Qin, A. Goldar, M. B. Wakin, Z. Zhu, and Z. Gong, arXiv preprint arXiv:2408.07115 (2024).

[53] J. I. Cirac, D. Perez-Garcia, N. Schuch, and F. Verstraete, *Reviews of Modern Physics* **93**, 045003 (2021).

[54] J. Haegeman, T. J. Osborne, H. Verschelde, and F. Verstraete, *Physical review letters* **110**, 100402 (2013).

[55] A. A. Mele, arXiv preprint arXiv:2307.08956 (2023).

[56] Z. Zhu, Q. Li, G. Tang, and M. B. Wakin, *IEEE Transactions on Information Theory* **67**, 1308 (2021).

[57] E. J. Candès, X. Li, Y. Ma, and J. Wright, *J. ACM* **58**, 1 (2011).

[58] S. Holtz, T. Rohwedder, and R. Schneider, *Numerische Mathematik* **120**, 701 (2012).

[59] Z. Qin, M. B. Wakin, and Z. Zhu, arXiv preprint arXiv:2401.02592 (2024).

[60] A. Zhang and D. Xia, *IEEE Transactions on Information Theory* **64**, 7311 (2018).

### Appendix A: Proof of Equation (4)

*Proof.* We expand  $\mathbb{E} \|\rho_{\text{CS}} - \rho^*\|_F^2$  as follows:

$$\begin{aligned}
\mathbb{E} \|\rho_{\text{CS}} - \rho^*\|_F^2 &= \mathbb{E} \left\| \frac{1}{M} \sum_{m=1}^M \rho_m - \rho^* \right\|_F^2 \\
&= \mathbb{E} \left\langle \frac{1}{M} \sum_{m=1}^M (\rho_m - \rho^*), \frac{1}{M} \sum_{m=1}^M (\rho_m - \rho^*) \right\rangle \\
&= \frac{1}{M^2} \mathbb{E} \sum_{m=1}^M \|\rho_m - \rho^*\|_F^2 \\
&= \frac{1}{M} \mathbb{E} \|\rho_1 - \rho^*\|_F^2 \\
&= \frac{1}{M} (\|\rho^*\|_F^2 - 2 \mathbb{E} \langle \rho_1, \rho^* \rangle + \mathbb{E} \langle \rho_1, \rho_1 \rangle) \\
&= \frac{1}{M} \left[ -\|\rho^*\|_F^2 + (2^n + 1)^2 \mathbb{E} \langle \phi_{1,j_1} \phi_{1,j_1}^\dagger, \phi_{1,j_1} \phi_{1,j_1}^\dagger \rangle - 2(2^n + 1) \mathbb{E} \langle \phi_{1,j_1} \phi_{1,j_1}^\dagger, \mathbf{I}_{2^n} \rangle + 2^n \right] \\
&= \frac{4^n + 2^n - 1 - \|\rho^*\|_F^2}{M}
\end{aligned} \tag{A1}$$

where the third line follows from  $\mathbb{E}[\rho_m] = \rho^*$ , the fourth from the equivalence under expectation of all measurements  $m$ , and the last from the normalization  $\langle \phi_{1,j_1} \phi_{1,j_1}^\dagger, \phi_{1,j_1} \phi_{1,j_1}^\dagger \rangle = \langle \phi_{1,j_1} \phi_{1,j_1}^\dagger, \mathbf{I}_{2^n} \rangle = 1$ .  $\square$

### Appendix B: Proof of Theorem 1

*Proof.* We define a restricted Frobenius norm as

$$\|\rho_{\text{PCS}} - \rho^*\|_{F, \widehat{\mathbb{X}}} = \|\rho_{\text{PCS}} - \rho^*\|_F = \max_{\rho \in \widehat{\mathbb{X}}} \langle \rho_{\text{PCS}} - \rho^*, \rho \rangle. \tag{B1}$$

Note that  $\widehat{\mathbb{X}}$ , includes conditions such as  $\text{trace}(\rho) = 0$ ,  $\rho = \rho^\dagger$  and  $\|\rho\|_F \leq 1$ . By the definition of the restricted Frobenius norm in Eq. (B1), we can further analyze

$$\|\rho_{\text{PCS}} - \rho^*\|_F = \|\rho_{\text{PCS}} - \rho^*\|_{F, \widehat{\mathbb{X}}} \leq \|\rho_{\text{CS}} - \rho^*\|_{F, \widehat{\mathbb{X}}} = \max_{\rho \in \widehat{\mathbb{X}}} \left\langle \frac{1}{M} \sum_{m=1}^M \left[ (2^n + 1) \phi_{m,j_m} \phi_{m,j_m}^\dagger - \mathbf{I}_{2^n} \right] - \rho^*, \rho \right\rangle, \tag{B2}$$

where the inequality follows from the assumption that the physical projection  $\mathcal{P}_{\mathbb{X}}(\cdot)$  is optimal and therefore satisfies nonexpansiveness. Next, we bound  $\frac{1}{M} \sum_{m=1}^M [(2^n + 1)\phi_{m,j_m} \phi_{m,j_m}^\dagger - \mathbf{I}_{2^n}] - \rho^*$  using the covering argument. According to the assumption, we initially construct an  $\epsilon$ -net  $\{\rho^{(1)}, \dots, \rho^{(N_\epsilon(\tilde{\mathbb{X}}))}\} \in \tilde{\mathbb{X}} \subset \hat{\mathbb{X}}$ , where the size of  $\tilde{\mathbb{X}}$  is denoted by  $N_\epsilon(\tilde{\mathbb{X}})$  such that

$$\sup_{\rho: \|\rho\|_F \leq 1} \min_{p \leq N_\epsilon(\tilde{\mathbb{X}})} \|\rho - \rho^{(p)}\|_F \leq \epsilon. \quad (\text{B3})$$

In addition, we denote  $\mathbf{B}_m = \frac{1}{M} ((2^n + 1)\phi_{m,j_m} \phi_{m,j_m}^\dagger - \mathbf{I}_{2^n} - \rho^*)$  and derive

$$\max_{\rho \in \tilde{\mathbb{X}}} \left\langle \sum_{m=1}^M \mathbf{B}_m, \rho \right\rangle = \max_{\rho \in \tilde{\mathbb{X}}} \left\langle \sum_{m=1}^M \mathbf{B}_m, \rho - \rho^{(p)} + \rho^{(p)} \right\rangle \leq \max_{\rho^{(p)} \in \tilde{\mathbb{X}}} \left\langle \sum_{m=1}^M \mathbf{B}_m, \rho^{(p)} \right\rangle + \epsilon \max_{\rho \in \tilde{\mathbb{X}}} \left\langle \sum_{m=1}^M \mathbf{B}_m, \rho \right\rangle.$$

By setting  $\epsilon = 0.5$  and moving the second term on the right-hand side to the left, we get

$$\max_{\rho \in \tilde{\mathbb{X}}} \left\langle \sum_{m=1}^M \mathbf{B}_m, \rho \right\rangle \leq \max_{\rho^{(p)} \in \tilde{\mathbb{X}}} 2 \left\langle \sum_{m=1}^M \mathbf{B}_m, \rho^{(p)} \right\rangle. \quad (\text{B4})$$

Then we need to build the concentration inequality for the right hand side of Eq. (B4). First, we define

$$\sum_{m=1}^M s_m = \sum_{m=1}^M \langle (2^n + 1)\phi_{m,j_m} \phi_{m,j_m}^\dagger - \mathbf{I}_{2^n} - \rho^*, \rho^{(p)} \rangle, \quad (\text{B5})$$

and due to  $\mathbb{E}[(2^n + 1)\phi_{m,j_m} \phi_{m,j_m}^\dagger - \mathbf{I}_{2^n} - \rho^*] = \mathbf{0}$ , we have  $\mathbb{E}[s_m] = 0$ . Moreover, we rewrite  $s_m$  as

$$\begin{aligned} s_m &= \langle (2^n + 1)\phi_{m,j_m} \phi_{m,j_m}^\dagger - \mathbf{I}_{2^n} - \rho^*, \rho^{(p)} \rangle \\ &= (2^n + 1) \left\langle \phi_{m,j_m} \phi_{m,j_m}^\dagger - \frac{\rho^*}{2^n + 1}, \rho^{(p)} \right\rangle \\ &= (2^n + 1) \left\langle \phi_{m,j_m} \phi_{m,j_m}^\dagger, \rho^{(p)} - \frac{\langle \rho^*, \rho^{(p)} \rangle}{2^n + 1} \mathbf{I}_{2^n} \right\rangle \\ &= (2^n + 1) \langle \phi_{m,j_m} \phi_{m,j_m}^\dagger, \mathbf{D} \rangle, \end{aligned} \quad (\text{B6})$$

where the second line follows from  $\text{trace}(\rho^{(p)}) = \langle \mathbf{I}_{2^n}, \rho^{(p)} \rangle = 0$ . We can further compute

$$\begin{aligned} \mathbb{E}[|s_m|^a] &= \mathbb{E}[(2^n + 1)^a |\langle \phi_{m,j_m} \phi_{m,j_m}^\dagger, \mathbf{D} \rangle|^a] \\ &\leq (2^n + 1)^a \mathbb{E}[(\text{trace}(\phi_{m,j_m} \phi_{m,j_m}^\dagger |\mathbf{D}|))^a] \\ &= \frac{(2^n + 1)^a}{C_{2^n+a-1}^a} \text{trace}(|\mathbf{D}|^{\otimes a} P_{\text{Sym}}) \\ &\leq \frac{(2^n + 1)^a}{C_{2^n+a-1}^a} \|\mathbf{D}\|_F^{\otimes a} \|P_{\text{Sym}}\| \\ &\leq 6 \times 2^{a-2} a!, \end{aligned} \quad (\text{B7})$$

where  $|\mathbf{D}| = \sqrt{\mathbf{D}^2} = \mathbf{U} \sqrt{\Sigma} \mathbf{V}^\dagger$  denotes the absolute value of the matrix  $\mathbf{D}$  with its compact SVD  $\mathbf{D}^2 = \mathbf{U} \Sigma \mathbf{V}^\dagger$  and  $\mathbf{A}^{\otimes a} = \underbrace{\mathbf{A} \otimes \dots \otimes \mathbf{A}}_a$  holds for any matrix  $\mathbf{A}$ . Given that the unitary Haar measure conforms to any unitary  $p$ -design, as exemplified in

Ref. [55, Example 51], we can deduce the third line, with  $P_{\text{Sym}}$  representing an orthogonal projector onto the symmetric subspace. The second inequality follows from [56, Lemma 7] and  $\|\mathbf{D}\|_F^{\otimes a} = \|\mathbf{D}^{\otimes a}\|_F$  due to the positive semidefiniteness of  $|\mathbf{D}|^{\otimes a}$  and the orthogonal projection. In the last line, we utilize  $\|\mathbf{D}\|_F \leq \|\rho^{(p)}\|_F + \|\frac{\langle \rho^*, \rho^{(p)} \rangle}{2^n + 1} \mathbf{I}_{2^n}\|_F \leq 1 + \frac{2^n}{2^n + 1} \|\rho^{(p)}\|_F \|\rho^*\|_F \leq 2$ ,  $\|P_{\text{Sym}}\| \leq 1$  and  $\frac{(2^n + 1)^a}{C_{2^n+a-1}^a} \leq \frac{3}{2} a!$ .

Based on Lemma 1 with  $\mathbb{E}[s_m] = 0$  and  $\mathbb{E}[|s_m|^a] \leq 6 \times 2^{a-2} a!$ , for any  $t \in [0, 1]$ , we have the probability

$$\mathbb{P} \left( \left| \frac{1}{M} \left\langle \sum_{m=1}^M \langle (2^n + 1)\phi_{m,j_m} \phi_{m,j_m}^\dagger - \mathbf{I}_{2^n} - \rho^*, \rho^{(p)} \rangle \right\rangle \right| \geq t \right) \leq 2e^{-\frac{Mt^2}{28}}. \quad (\text{B8})$$

Combining Eqs. (B4,B8), there exists an  $\epsilon$ -net  $\tilde{\mathbb{X}}$  of  $\mathbb{X}$  such that

$$\begin{aligned}
\mathbb{P} \left( \max_{\rho \in \tilde{\mathbb{X}}} \left\langle \frac{1}{M} \sum_{m=1}^M \left[ (2^n + 1) \phi_{m,j_m} \phi_{m,j_m}^\dagger - \mathbf{I}_{2^n} \right] - \rho^*, \rho \right\rangle \geq t \right) &\leq \mathbb{P} \left( \max_{\rho^{(p)} \in \tilde{\mathbb{X}}} \frac{1}{M} \sum_{m=1}^M \langle (2^n + 1) \phi_{m,j_m} \phi_{m,j_m}^\dagger - \mathbf{I}_{2^n} - \rho^*, \rho^{(p)} \rangle \geq \frac{t}{2} \right) \\
&\leq \mathbb{P} \left( \max_{\rho^{(p)} \in \tilde{\mathbb{X}}} \frac{1}{M} \left| \sum_{m=1}^M \langle (2^n + 1) \phi_{m,j_m} \phi_{m,j_m}^\dagger - \mathbf{I}_{2^n} - \rho^*, \rho^{(p)} \rangle \right| \geq \frac{t}{2} \right) \\
&\leq 2N_\epsilon(\tilde{\mathbb{X}}) e^{-\frac{Mt^2}{112}} \\
&\leq e^{-\frac{Mt^2}{112} + \log 2N_\epsilon(\tilde{\mathbb{X}})}. \tag{B9}
\end{aligned}$$

We opt for  $t = O\left(\sqrt{\frac{\log N_\epsilon(\tilde{\mathbb{X}})}{M}}\right)$ , and subsequently, with probability  $1 - e^{-\Omega(\log N_\epsilon(\tilde{\mathbb{X}}))}$ , we derive

$$\|\rho_{\text{PCS}} - \rho^*\|_F \leq O\left(\sqrt{\frac{\log N_\epsilon(\tilde{\mathbb{X}})}{M}}\right). \tag{B10}$$

□

### Appendix C: Proof of Theorem 3

*Proof.* We define a restricted Frobenius norm as following:

$$\|\rho_1 - \rho_2\|_{F,2r} = \|\rho_1 - \rho_2\|_F = \max_{\rho \in \tilde{\mathbb{X}}_{2r}} \langle \rho_1 - \rho_2, \rho \rangle, \tag{C1}$$

where the set  $\tilde{\mathbb{X}}_r$  is defined as follows:

$$\tilde{\mathbb{X}}_r = \{\rho \in \mathbb{C}^{2^n \times 2^n} : \rho = \rho^\dagger, \text{rank}(\rho) = r, \text{trace}(\rho) = 0, \|\rho\|_F \leq 1\}. \tag{C2}$$

By the definition of the restricted Frobenius norm in Eq. (C1), we can further analyze

$$\begin{aligned}
\|\rho_{\text{LR-PCS}} - \rho^*\|_F &= \|\rho_{\text{LR-PCS}} - \rho^*\|_{F,2r} \\
&\leq \|\mathcal{P}_{\text{ED}}(\rho_{\text{CS}}) - \rho^*\|_{F,2r} \\
&\leq 2\|\rho_{\text{CS}} - \rho^*\|_{F,2r} \\
&= 2 \max_{\rho \in \tilde{\mathbb{X}}_{2r}} \left\langle \frac{1}{M} \sum_{m=1}^M \left[ (2^n + 1) \phi_{m,j_m} \phi_{m,j_m}^\dagger - \mathbf{I}_{2^n} \right] - \rho^*, \rho \right\rangle, \tag{C3}
\end{aligned}$$

where the first two inequalities respectively follow the nonexpansiveness property of the projection and the quasi-optimality property of eigenvalue decomposition (ED) projection [40]. Next, we need bound the first term in the last line of Eq. (C3) using the covering argument. According to Ref. [57, Lemma 3.1], we initially construct an  $\epsilon$ -net  $\{\rho^{(1)}, \dots, \rho^{N_\epsilon(\tilde{\mathbb{X}}_{2r})}\} \in \tilde{\mathbb{X}}_{2r} \subset \tilde{\mathbb{X}}_{2r}$  in which the size of  $\tilde{\mathbb{X}}_{2r}$  is denoted by  $N_\epsilon(\tilde{\mathbb{X}}_{2r}) \leq \left(\frac{9}{\epsilon}\right)^{(2^{n+2}+2)r}$  such that

$$\sup_{\rho: \|\rho\|_F \leq 1} \min_{p \leq N_\epsilon(\tilde{\mathbb{X}}_{2r})} \|\rho - \rho^{(p)}\|_F \leq \epsilon. \tag{C4}$$

Combining Eqs. (B4,B8) in Appendix B, there exists an  $\epsilon$ -net  $\tilde{\mathbb{X}}_{2r}$  of  $\tilde{\mathbb{X}}_{2r}$  such that

$$\begin{aligned}
\mathbb{P} \left( \max_{\rho \in \tilde{\mathbb{X}}_{2r}} \left\langle \frac{1}{M} \sum_{m=1}^M \left[ (2^n + 1) \phi_{m,j_m} \phi_{m,j_m}^\dagger - \mathbf{I}_{2^n} \right] - \rho^*, \rho \right\rangle \geq t \right) &\leq \mathbb{P} \left( \max_{\rho^{(p)} \in \tilde{\mathbb{X}}_{2r}} \frac{1}{M} \sum_{m=1}^M \langle (2^n + 1) \phi_{m,j_m} \phi_{m,j_m}^\dagger - \mathbf{I}_{2^n} - \rho^*, \rho^{(p)} \rangle \geq \frac{t}{2} \right) \\
&\leq \mathbb{P} \left( \max_{\rho^{(p)} \in \tilde{\mathbb{X}}_{2r}} \frac{1}{M} \left| \sum_{m=1}^M \langle (2^n + 1) \phi_{m,j_m} \phi_{m,j_m}^\dagger - \mathbf{I}_{2^n} - \rho^*, \rho^{(p)} \rangle \right| \geq \frac{t}{2} \right) \\
&\leq 2 \left( \frac{9}{\epsilon} \right)^{(2^{n+2}+2)r} e^{-\frac{Mt^2}{112}} \\
&\leq e^{-\frac{Mt^2}{112} + C2^n r}, \tag{C5}
\end{aligned}$$

where we set  $\epsilon = \frac{1}{2}$  and  $C$  is a positive constant. We opt for  $t = O\left(\sqrt{\frac{2^n r}{M}}\right)$  and subsequently, with probability  $1 - e^{-\Omega(2^n r)}$ , derive

$$\|\rho_{\text{LR-PCS}} - \rho^*\|_F \leq O\left(\sqrt{\frac{2^n r}{M}}\right). \quad (\text{C6})$$

□

#### Appendix D: Proof of Theorem 4

We define a restricted Frobenius norm as following:

$$\|\rho_1 - \rho_2\|_{F,2D} = \|\rho_1 - \rho_2\|_F = \max_{\rho \in \widehat{\mathbb{X}}_{2D}} \langle \rho_1 - \rho_2, \rho \rangle. \quad (\text{D1})$$

where we denote by  $\widehat{\mathbb{X}}_D$  the normalized set of MPOs with bond dimension  $D$ :

$$\widehat{\mathbb{X}}_D = \left\{ \rho \in \mathbb{C}^{2^n \times 2^n} : \rho = \rho^\dagger, \|\rho\|_F \leq 1, \text{trace}(\rho) = 0, \text{bond dimension}(\rho) = D \right\}. \quad (\text{D2})$$

Note that the presence of additional orthonormal structures arises from the fact that, according to Ref. [58], any TT form is equivalent to a left-orthogonal TT form [40].

We define  $\mathcal{P}_{\text{trace}}(\cdot)$  as a projection onto convex set  $\{\rho \in \mathbb{C}^{2^n \times 2^n} : \text{trace}(\rho) = 1\}$ . By the definition of the restricted Frobenius norm (D1), we can derive

$$\begin{aligned} \|\rho_{\text{MPO-PCS}} - \rho^*\|_F &\leq \|\mathcal{P}_{\text{trace}}(\text{SVD}_D^{tt}(\rho_{\text{CS}})) - \rho^*\|_F \\ &= \|\mathcal{P}_{\text{trace}}(\text{SVD}_D^{tt}(\rho_{\text{CS}})) - \rho^*\|_{F,2D} \\ &\leq \|\text{SVD}_D^{tt}(\rho_{\text{CS}}) - \rho^*\|_{F,2D} \\ &\leq (1 + \sqrt{n-1}) \|\rho_{\text{CS}} - \rho^*\|_{F,2D} \\ &= (1 + \sqrt{n-1}) \max_{\rho \in \widehat{\mathbb{X}}_{2D}} \left\langle \frac{1}{M} \sum_{m=1}^M ((2^n + 1) \phi_{m,j_m} \phi_{m,j_m}^\dagger - \mathbf{I}_{2^n}) - \rho^*, \rho \right\rangle \\ &= (1 + \sqrt{n-1}) \max_{\rho \in \widehat{\mathbb{X}}_{2D}} \left\langle \frac{1}{M} \sum_{m=1}^M ((2^n + 1) \phi_{m,j_m} \phi_{m,j_m}^\dagger - \mathbf{I}_{2^n}) - \rho^*, \rho \right\rangle \end{aligned} \quad (\text{D3})$$

where the first two inequalities respectively follow from the nonexpansiveness property of the projection onto the convex set, while the third inequality is a consequence of the quasi-optimality property of TT-SVD projection [40]. Additionally, we denote

$$\begin{aligned} \widehat{\mathbb{X}}_D = \left\{ \rho \in \mathbb{C}^{2^n \times 2^n} : \rho = \rho^\dagger, \text{trace}(\rho) = 0, \rho(i_1 \cdots i_n, j_1 \cdots j_n) = \mathbf{X}_1^{i_1,j_1} \mathbf{X}_2^{i_2,j_2} \cdots \mathbf{X}_n^{i_n,j_n}, \right. \\ \left. \mathbf{X}_1^{i_1,j_1} \in \mathbb{C}^{1 \times D}, \mathbf{X}_n^{i_n,j_n} \in \mathbb{C}^{D \times 1}, \mathbf{X}_\ell^{i_\ell,j_\ell} \in \mathbb{C}^{D \times D}, \|L(\mathbf{X}_\ell)\| \leq 1, \ell \in [n-1], \|L(\mathbf{X}_n)\|_F \leq 1 \right\}. \end{aligned} \quad (\text{D4})$$

Based on  $\|\rho\|_F = \|L(\mathbf{X}_n)\|_F \leq 1$  for a left-orthogonal TT form using [59, Eq.(44)], we obtain the last line.

Next, we will apply the covering argument to bound (D3). For any fixed value of  $\tilde{\rho} \in \tilde{\mathbb{X}}_{2D} \subset \widehat{\mathbb{X}}_{2D}$ , using Eq. (B4), concentration inequality in Eq. (B8) and Lemma 3, there exists an  $\epsilon$ -net  $\tilde{\mathbb{X}}_{2D}$  of  $\widehat{\mathbb{X}}_{2D}$  such that

$$\begin{aligned} \mathbb{P} \left( \max_{\rho \in \tilde{\mathbb{X}}_{2D}} \left\langle \frac{1}{M} \sum_{m=1}^M ((2^n + 1) \phi_{m,j_m} \phi_{m,j_m}^\dagger - \mathbf{I}_{2^n}) - \rho^*, \rho \right\rangle \geq t \right) &\leq \mathbb{P} \left( \max_{\tilde{\rho} \in \tilde{\mathbb{X}}_{2D}} \frac{1}{M} \sum_{m=1}^M \left\langle (2^n + 1) \phi_{m,j_m} \phi_{m,j_m}^\dagger - \mathbf{I}_{2^n} - \rho^*, \tilde{\rho} \right\rangle \geq \frac{t}{2} \right) \\ &\leq \mathbb{P} \left( \max_{\tilde{\rho} \in \tilde{\mathbb{X}}_{2D}} \frac{1}{M} \left| \sum_{m=1}^M \left\langle (2^n + 1) \phi_{m,j_m} \phi_{m,j_m}^\dagger - \mathbf{I}_{2^n} - \rho^*, \tilde{\rho} \right\rangle \right| \geq \frac{t}{2} \right) \\ &\leq 2 \left( \frac{4n + \epsilon}{\epsilon} \right)^{4nD^2} e^{-\frac{Mt^2}{112}} \\ &\leq e^{-\frac{Mt^2}{112} + CnD^2 \log n}, \end{aligned} \quad (\text{D5})$$

where we set  $\epsilon = \frac{1}{2}$  and  $C$  is a positive constant. We opt for  $t = O\left(\sqrt{\frac{nD^2 \log n}{M}}\right)$  and subsequently, with probability  $1 - e^{-\Omega(nD^2 \log n)}$ , derive

$$\|\rho_{\text{MPO-PCS}} - \rho^*\|_F \leq O\left(\sqrt{\frac{n^2 D^2 \log n}{M}}\right). \quad (\text{D6})$$

### Appendix E: Auxiliary Materials

**Lemma 1.** (Classical Bernstein's inequality [23, Theorem 6]) Let  $s_1, \dots, s_n \in \mathbb{R}$  denote i.i.d. copies of a mean-zero random variable  $s$  that obeys  $\mathbb{E}[|s|^p] \leq p!R^{p-2}\sigma^2/2$  for all integers  $p \geq 2$ , where  $R, \sigma^2 > 0$  are constants. Then, for all  $t > 0$ ,

$$\mathbb{P}\left(\left|\sum_{i=1}^n s_i\right| \geq t\right) \leq 2e^{-\frac{t^2/2}{n\sigma^2+Rt}}. \quad (\text{E1})$$

**Lemma 2.** ([30, Lemma 10]) For any  $\mathbf{A}_i, \mathbf{A}_i^* \in \mathbb{R}^{r_{i-1} \times r_i}$ ,  $i \in \{1, \dots, N\}$ , we have

$$\mathbf{A}_1 \mathbf{A}_2 \cdots \mathbf{A}_N - \mathbf{A}_1^* \mathbf{A}_2^* \cdots \mathbf{A}_N^* = \sum_{i=1}^N \mathbf{A}_1^* \cdots \mathbf{A}_{i-1}^* (\mathbf{A}_i - \mathbf{A}_i^*) \mathbf{A}_{i+1} \cdots \mathbf{A}_N. \quad (\text{E2})$$

**Lemma 3.** There exists an  $\epsilon$ -net  $\tilde{\mathbb{X}}_D$  for  $\hat{\mathbb{X}}_D$  in Eq. (D4) under the Frobenius norm, i.e.,  $\|\rho - \rho^{(p)}\|_F \leq \epsilon$  for  $\rho^{(p)} \in \tilde{\mathbb{X}}_D$ , obeying

$$N_\epsilon(\tilde{\mathbb{X}}_D) \leq \left(\frac{4n + \epsilon}{\epsilon}\right)^{4nD^2}, \quad (\text{E3})$$

where  $N_\epsilon(\tilde{\mathbb{X}}_D)$  denotes the number of elements in the set  $\tilde{\mathbb{X}}_D$ .

*Proof.* For each set of matrices  $\{L(\mathbf{X}_\ell) \in \mathbb{R}^{4D \times D} : \|L(\mathbf{X}_\ell)\| \leq 1\}$ , according to Ref. [60], we can construct an  $\xi$ -net  $\{L(\mathbf{X}_\ell^{(1)}), \dots, L(\mathbf{X}_\ell^{(N_\ell)})\}$  with the covering number  $N_\ell \leq (\frac{4+\xi}{\xi})^{4D^2}$  such that

$$\sup_{L(\mathbf{X}_\ell) : \|L(\mathbf{X}_\ell)\| \leq 1} \min_{p_\ell \leq N_\ell} \|L(\mathbf{X}_\ell) - L(\mathbf{X}_\ell^{(p_\ell)})\| \leq \xi, \quad (\text{E4})$$

for all  $\ell \in \{1, \dots, n-1\}$ . Also, we can construct an  $\xi$ -net  $\{L(\mathbf{X}_n^{(1)}), \dots, L(\mathbf{X}_n^{(N_n)})\}$  for  $\{L(\mathbf{X}_n) \in \mathbb{R}^{4D \times 1} : \|L(\mathbf{X}_n)\|_F \leq 1\}$  such that

$$\sup_{L(\mathbf{X}_n) : \|L(\mathbf{X}_n)\|_F \leq 1} \min_{p_n \leq N_n} \|L(\mathbf{X}_n) - L(\mathbf{X}_n^{(p_n)})\|_F \leq \xi, \quad (\text{E5})$$

with the covering number  $N_n \leq (\frac{2+\xi}{\xi})^{4D}$ .

Therefore, we can construct a  $\xi$ -net  $\{[\mathbf{X}_1^{(1)}, \dots, \mathbf{X}_n^{(1)}], \dots, [\mathbf{X}_1^{(N_1)}, \dots, \mathbf{X}_n^{(N_n)}]\}$  with covering number

$$\prod_{\ell=1}^n N_\ell \leq \left(\frac{4+\xi}{\xi}\right)^{4nD^2} \quad (\text{E6})$$

for any MPO  $\rho = [\mathbf{X}_1, \dots, \mathbf{X}_n]$  with bond dimension  $D$ . Then we expand  $\|\rho - \rho^{(p)}\|_F$  as follows:

$$\begin{aligned} \|\rho - \rho^{(p)}\|_F &= \|[\mathbf{X}_1, \dots, \mathbf{X}_n] - [\mathbf{X}_1^{(p_1)}, \dots, \mathbf{X}_n^{(p_n)}]\|_F \\ &= \left\| \sum_{a_l=1}^n [\mathbf{X}_1^{(p_1)}, \dots, \mathbf{X}_{a_l-1}^{(p_l)}, \mathbf{X}_{a_l}^{(p_{a_l})} - \mathbf{X}_{a_l}, \mathbf{X}_{a_l+1}, \dots, \mathbf{X}_n] \right\|_F \\ &\leq \sum_{a_l=1}^n \|[\mathbf{X}_1^{(p_1)}, \dots, \mathbf{X}_{a_l-1}^{(p_l)}, \mathbf{X}_{a_l}^{(p_{a_l})} - \mathbf{X}_{a_l}, \mathbf{X}_{a_l+1}, \dots, \mathbf{X}_n]\|_F \\ &\leq \sum_{a_l=1}^{n-1} \|L(\mathbf{X}_{a_l}^{(p_{a_l})}) - L(\mathbf{X}_{a_l})\| + \|L(\mathbf{X}_n^{(p_n)}) - L(\mathbf{X}_n)\|_F \\ &\leq n\xi = \epsilon, \end{aligned}$$

where the second line and the second inequality respectively follow Lemma 2 and [30, Eq.(47)]. In addition, we choose  $\xi = \frac{\epsilon}{n}$  in the last line. Ultimately, we can construct an  $\epsilon$ -net  $\{\rho^{(1)}, \dots, \rho^{N_1 \dots N_n}\}$  with covering number

$$N_\epsilon(\tilde{\mathbb{X}}_D) \leq \left( \frac{4n + \epsilon}{\epsilon} \right)^{4nD^2} \quad (\text{E7})$$

for any MPO  $\rho \in \tilde{\mathbb{X}}_D$ . □